Decarboxylation-Induced Cross-Linking of a Polyimide for Enhanced CO_2 Plasticization Resistance

Adam M. Kratochvil and William J. Koros*

School of Chemical & Biomolecular Engineering, Georgia Institute of Technology, Atlanta, Georgia 30332-0100

Received July 14, 2008; Revised Manuscript Received September 15, 2008

ABSTRACT: A novel cross-linking approach for a carboxylic acid-containing 6FDA-based copolyimide is presented and characterized. This new type of cross-linking renders the polyimide insoluble in typical solvents and greatly enhances the resistance to plasticization under high CO_2 pressure. Charge transfer complexing, oligomer cross-linking, decomposition, and dianhydride formation are all ruled out as possible causes of these enhanced properties. Rather, high thermal annealing temperatures decarboxylate the pendant acid group which creates a phenyl radical capable of attacking other portions of the polyimide for cross-linking. CO_2 permeation isotherms reveal the enhanced stability against plasticization, and IR and C NMR confirm the evolution of CO_2 and loss of the carbonyl carbon from the polymer as a result of the cross-linking.

Introduction

It is well-known that polyimides have exceptional gas separation properties. Selected members in this family that have both "stiff" backbones and packing-inhibited groups within the backbone create an attractive distribution of free volume for performing subtle size and shape discrimination between similarly sized penetrants.[1] Polyimides have shown promise as a membrane material for use in aggressive feed separations, such as natural gas purification with a high CO_2 content, due to their robust mechanical properties, high glass transition temperatures, and resistance to chemical breakdown. However, at high pressures, CO_2 tends to plasticize, or swell, polymer membranes which greatly diminishes the separating efficiency of the membrane. Recent work demonstrates that cross-linking a polyimide membrane increases the pressure at which plasticization occurs, thus stabilizing the membrane at higher pressures of CO_2.[2−4] The diol cross-linking agents used in this earlier work formed ester linkages through a carboxylic acid pendant group, thus preserving the imide backbone and the high gas permeabilities associated with polyimides.[2,5,6] However, these ester linkages can potentially be hydrolyzed in aggressive acid gas feed streams which would reverse the effects of cross-linking and greatly reduce the efficiency of the membrane.

In this work, the same carboxylic acid containing base polyimide from the previous work is used; however, the discovery of a new cross-linking approach is presented which results in a covalently cross-linked polymer that lacks these vulnerable ester linkages. This new cross-linking mechanism occurs through the decarboxylation of the acid pendant at high temperatures and creates free radical sites capable of cross-linking without the diol cross-linking agent used in previous work.

Background

Gas transport through a membrane can be characterized by the permeability coefficient (P_A), which is defined as the pressure and thickness normalized flux across the membrane:

$$P_A = \frac{N_A l}{\Delta p_A}$$

In this equation, N_A is the flux of component A through the membrane, l is the membrane thickness, and Δp_A is the difference in partial pressure of A acting across the membrane. The units of the permeability coefficient are generally defined as barrers according to the following relationship:

$$1\ \text{barrer} = 10^{-10}\ \frac{\text{cm}^3\ (\text{STP})\ \text{cm}}{\text{cm}^2\ \text{s}\ \text{cmHg}}$$

At low pressures, permeability decreases with increasing pressure due to the filling of Langmuir sorption sites. However, at higher pressures, the contribution of the Langmuir region to the overall permeability diminishes and gas permeability approaches a constant value associated with simple dissolution (Henry's law) transport. This response is known as a dual mode permeation response.[7] However, for more strongly sorbing and interacting penetrants like CO_2, the polymer eventually exhibits an upswing in the permeation isotherm due to swelling-induced plasticization. The pressure at which this upturn occurs is often referred to as the "plasticization pressure". On the molecular scale level, plasticization is believed to occur when the presence of the penetrant enhances segmental motion of the polymer chains. This increase in segmental motion allows for a greater frequency and size of transient intersegmental gaps, leading to a higher diffusion coefficient. Plasticization is detrimental to gas pair separations relying upon mobility selectivity, since it enables easier diffusion of the larger penetrant with respect to the smaller penetrant.

Experimental Section

The copolyimide used in this work is 6FDA-DAM:DABA (2:1), shown in Figure 1, and is further referred to as the "free acid" polymer due to the open carboxylic acid groups on the DABA moiety. Packing inhibitions due to the DAM moiety provide considerable free volume, which enhances the productivity of the membrane for natural gas separations. On the other hand, the DABA moiety provides a carboxylic acid pendant group which can be used to cross-link the polymer. This polyimide was synthesized through a two-step polycondensation reaction. In the first step, stoichiometric

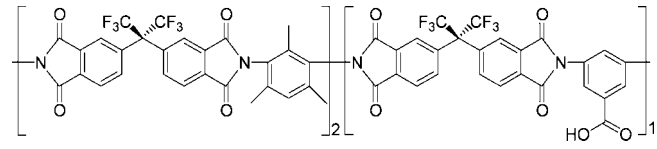

Figure 1. 6FDA-DAM:DABA (2:1) structure.

* Corresponding author. E-mail: William.Koros@chbe.gatech.edu.

10.1021/ma801586f CCC: $40.75
Published on Web 10/16/2008

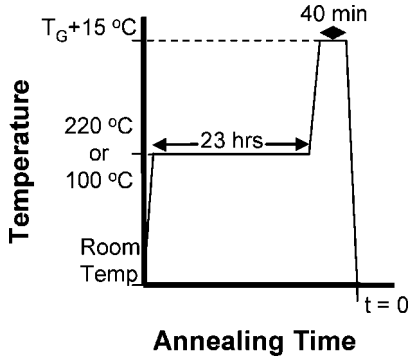

Figure 2. Thermal annealing profiles for the 6FDA-DAM:DABA (2:1) free acid films. Annealing protocol 1 refers to the 100 °C sub-T_G drying step, and annealing protocol 2 refers to the 220 °C sub-T_G drying step.

amounts of the three monomers were added to NMP at room temperature to make a 20 wt % solution. This solution was stirred at room temperature for 18 h to produce the polyamic acid. The second step involves heating the highly viscous solution to 200 °C for 24 h to close the imide ring and complete the imidization of the polymer. At the beginning of this step, *o*-dichlorobenzene was added to the solution and allowed to reflux into a Dean−Stark trap to facilitate the removal of water which can cleave the amide bond and reduce molecular weight. Great care was taken to remove water from all aspects of the synthesis to further the reactions and prevent chain scissioning. This was done through drying all chemicals over dried molecular sieves, drying the monomer before addition, flaming and purging all glassware, and maintaining a pure N_2 purge during all steps of the reactions. IR spectroscopy confirmed the elimination of the amide peak following the thermal imidization procedure. Once imidization was complete, the solution was precipitated into a 50/50 water/methanol mixture to phase separate the polymer. The polymer was then blended and washed multiple times with the water/methanol solution at room temperature to remove as much NMP as possible.

Thick, dense polymer films were solution cast into a Teflon mold in a controlled environment glovebag. The glovebag was purged with pure nitrogen for 15 min to remove water and then saturated with THF from an open jar within the bag for 15 min. A 5 wt % polymer solution in THF was then filtered with a syringe through a 0.20 μm PTFE filter into the mold. The mold was covered with a glass dish to reduce the rate of THF evaporation. Approximately 24 h later, the film was vitrified and could be removed from the glovebag. Film thicknesses for this study were ∼50 μm. Gas permeation measurements in this work were acquired using constant-volume, variable-pressure systems which were operated at 35 °C.

Polymer film samples for gas permeation and solvent dissolution tests were annealed above the glass transition temperature using a controlled procedure and environment. The glass transition temperature for this copolyimide was determined to be 374 °C from differential scanning calorimetry measurements, which agrees well with literature values for this same polymer.[8,9] Because the glass transition temperature is so high, a Thermcraft split-tube furnace was outfitted with an internal thermocouple for temperature control and a helium purge to create an inert annealing environment. The furnace tube was purged with at least 10 times its volume prior to thermal annealing, and the helium purge was maintained at ∼50 sccm/min during the annealing process. All samples were annealed in a free-standing state by hanging the sample with copper wire from a stainless steel support. The thermal annealing procedures, shown in Figure 2, include a sub-T_G drying step at either 100 or 220 °C for 23 h to remove any residual solvent followed by a rapid ramp to 15 deg above T_G (389 °C) for 40 min. At the 40 min mark, the films were rapidly quenched to room temperature through immediate removal from the furnace, which took approximately 2−4 s.

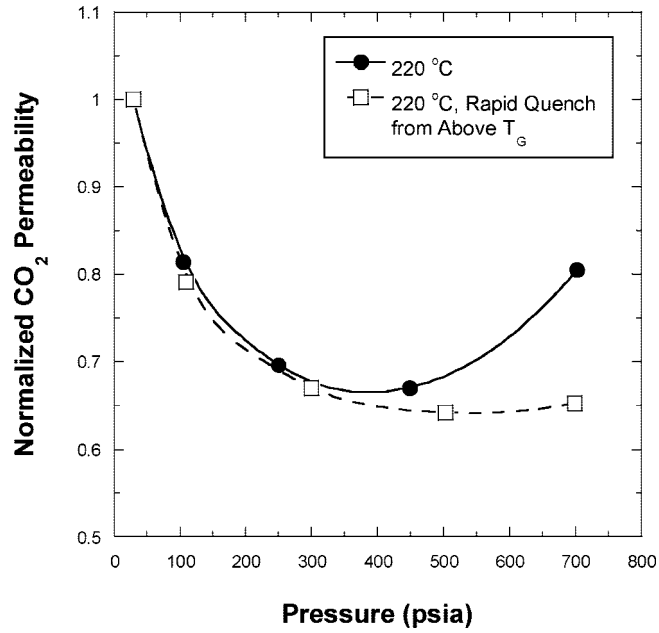

Figure 3. Normalized CO_2 permeation isotherms for 6FDA-DAM:DABA (2:1) free acid films annealed at 220 °C for 23 h and annealed at 220 °C for 23 h followed by rapid quenching from above T_G. The curves are to guide the eye.

Examination of the polymer during the annealing process was conducted using thermogravimetric analysis with the ability to be coupled with IR for evolved gas determination. The TGA was a Netzsch STA 409PC instrument, and all samples were run under an inert N_2 purge of 30 mL/min. The temperature profiles are displayed with the mass loss data. For IR measurements, a Bruker Tensor 27 with a resolution of 4 cm^{-1} and at least 64 scans was used to measure either polymer samples or evolved gases from the TGA.

Fluorescence spectroscopy and solid-state carbon NMR were employed to examine the polymer following the high-temperature thermal treatment. A CRAIC 1000 spectrometer using a 50× objective at 365 nm was used for fluorescence measurements, and a Bruker DSX 300 was used for NMR measurements.

Results

Because quenching a polymer film from above T_G introduces large amounts of excess free volume into the polymer matrix, gas permeabilities in the quenched film will be significantly larger than an as-cast or annealed film of the same material. Therefore, in order to compare a quenched sample with a control sample, gas permeabilities are normalized with respect to the initial permeability measurement at 2 atm. Figure 3 displays a CO_2 permeability isotherm for the free acid polymer film quenched from above T_G using protocol 2 and a control sample annealed at 220 °C for 23 h. A typical plasticization response for this polymer is observed in the control sample with a plasticization pressure of 400 psia, whereas the sample quenched from above T_G exhibits enhanced plasticization resistance. To determine whether this enhanced resistance is simply a result of introducing more excess free volume into the polymer, quenched samples were placed in typical solvents used for casting this polyimide into films, such as cyclohexanone, THF, and NMP. For all three solvents, none of the quenched samples redissolved. In fact, a free acid film quenched from above T_G remained insoluble after boiling in NMP for 18 h. These two responses indicate some form of cross-linking is occurring, whether physical or chemical; however, the free acid polyimide lacks the diol cross-linking agent typically used to cross-link this polymer.

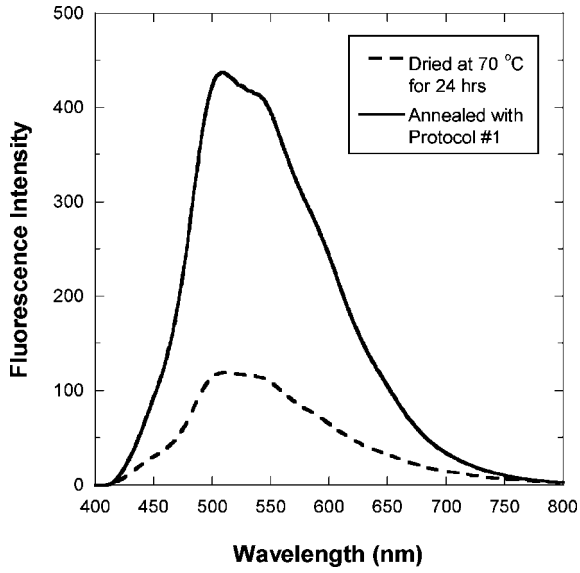

Figure 4. Fluorescence spectra of a dried and thermally quenched 6FDA-DAM:DABA (2:1) free acid sample.

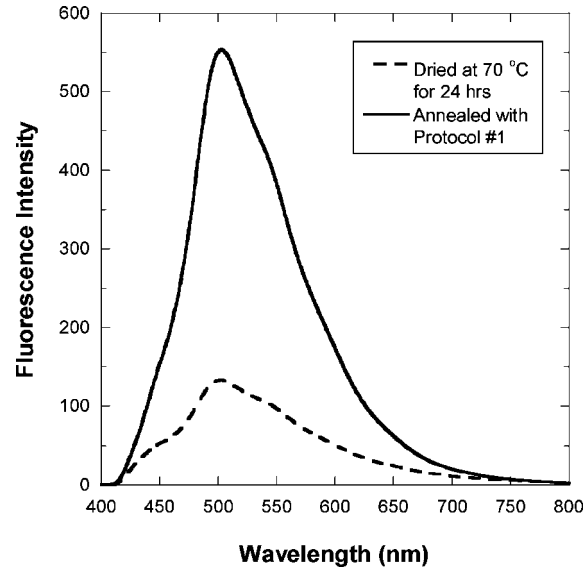

Figure 5. Fluorescence spectra of a dried and thermally quenched 6FDA-DAM sample.

There are a few possible explanations for these responses of the free acid quenched from above T_G which will be explored. First, this polymer is capable of forming charge transfer complexes which has been shown to stabilize another polyimide against plasticization.[10−12] This stabilization may also lead to greater insolubility in typical solvents. From a thermodynamic standpoint, when the polymer is in the rubbery region during the annealing process, enhanced chain mobility will allow alignment of the necessary components to form these complexes which results in an energetically more favorable state. Second, thermal degradation of similar polyimides has been shown to create a carbon structure with enhanced gas separation properties.[13−15] This new material should be resistant to penetrant swelling since it consists of a rigid, ultramicroporous carbon structure. The T_G of the free acid is sufficiently high (374 °C) that the beginning stages of polymer degradation may be occurring which could lead to these stabilization effects. Finally, even though this free acid polymer is considered to be "non-cross-linkable", i.e., it does not have the glycol cross-linking agent chemically attached to the DABA acid site, the high annealing temperature may cause some form of chemical reaction or reorganization to occur, which could then stabilize the polymer.

Investigation of Charge Transfer Complexes. Figure 4 presents fluorescence spectra of a free acid film dried at 70 °C for 24 h and a film annealed using protocol 1. Each curve is a representation of three different measurements per sample. The samples used for these measurements are adjacent samples from the same cast film, and both samples were measured on the spectrometer at the same time to eliminate the issue of changes in instrument calibration over time. As a complementary measurement, a structurally similar polymer, 6FDA-DAM, was examined with fluorescence spectroscopy in the same manner as described above with the results shown in Figure 5, and solubility tests were performed in THF and NMP. Even though this polymer is structurally different than the free acid, rapid quench from 389 °C increased the film thickness from 33 to 74 μm. This response is indicative of a polymer film surpassing the glassy transition followed by a rapid quench to room temperature.[16] Surprisingly, solubility tests revealed the 6FDA-DAM polymer to be soluble in both THF and NMP at room temperature following the high-temperature treatment.

These data reveal many insights into annealing the free acid above T_G. As mentioned before, when in the rubbery state, these polymers are expected to form charge transfer complexes which leads to a more favorable energy state. The fluorescence spectra for both the 6FDA-DAM:DABA (2:1) and 6FDA-DAM confirm this hypothesis as shown by the 4-fold increase in fluorescence intensity when quenched from above T_G. Also, the 6FDA-DAM solubility in THF and NMP following thermal treatment demonstrates that charge transfer complexes are not sufficiently strong enough to stabilize these polymers against strong swelling or even dissolving in these solvents. Ultimately, these data reveal that charge transfer complexes are not the cause of the insolubility and enhanced plasticization resistance of the free acid, and the DABA moiety of the free acid is most likely responsible for these effects following the rapid quench from above T_G.

Investigation of Oligomer Cross-Linking. Previous work has explored the ability to cross-link polyimides with both small and large molecule diamines.[17−20] While the polymer film is immersed in a methanol/diamine solution at room temperature, the diamines cleave the imide ring and form an amide linkage on the polymer backbone. The opposite end of the diamine then reacts with another imide ring in a similar manner. The result is a cross-linked polymer through the newly formed amides. The purpose of the methanol is to swell the polymer to enhance the chain mobility which allows alignment for the cross-links to form. When the large batch of 6FDA-DAM:DABA (2:1) free acid was synthesized and analyzed with GPC, a small secondary distribution existed in the low molecular weight region, indicating material with a low degree of polymerization is present in the bulk polymer. Based on the polystyrene calibration, this low molecular weight material is equivalent to 1−3 repeat unit oligomers. If these small chain oligomers contain amine end groups, either DAM or DABA substituents, it is reasonable to conclude that the high-temperature annealing above T_G provides enough polymer mobility to form the amide cross-links mentioned above. To test this possibility, the low molecular weight polymer was removed from a small batch of the free acid, and the remaining high molecular weight polymer was heat treated using protocol 2 and examined with solubility tests and gas permeation.

A small batch of the free acid was placed in a near-Θ solvent (50/50 THF/methanol) and mixed for 18 h to greatly swell the polymer and dissolve the low molecular weight species. The remaining polymer was then placed in a fresh 50/50 THF/methanol solution and mixed again for 18 h. Once removed

Table 1. Molecular Weight Information for the Washed and Extracted Free Acid Polymer

polymer	M_n	PDI
washed free acid	78337	1.904
extracted free acid	912	4.449

and dried, ~75% of the polymer remained. Both the washed and extracted polymer were examined with GPC to determine the efficiency of the extraction. The washed polymer contains only high molecular weight material, whereas the extracted polymer contains a mix of high and low molecular weight material. The molecular weight values and PDI for each are presented in Table 1.

Upon thermal treatment with protocol 2, the high molecular weight polymer remains insoluble in both THF and NMP. Furthermore, as shown in Figure 6, after rapid quenching from above T_G, the CO_2 plasticization resistance of the washed free acid is nearly identical to the original free acid. Therefore, the small chain oligomers that are present in the original free acid polymer are not responsible for the cross-linking effects that are observed following rapid quench from above T_G.

Decomposition of the Free Acid. TGA measurements coupled with IR of the evolved gases were conducted on the free acid polymer to characterize the decomposition of the polymer. The temperature was ramped up to 800 °C at a rate of 5 °C/min in a nitrogen purge. Figure 7 displays the mass loss of the polymer and temperature profile of the measurement. The first mass loss begins at 80 °C and can be attributed to water evolution and possibly trace amounts of residual solvent since mass loss continues until ~220 °C. There is also a second mass loss between 350 and 415 °C which will be addressed later. The significant mass loss associated with polymer decomposition begins at 470 °C. Figure 8 displays the 3-D IR spectra of gas evolution, and Figure 9 displays the IR trace at 1150 cm^{-1} which corresponds to HCF_3 evolution which has been determined to be one of the first byproducts of decomposition in similar polyimides.[21] The large, growing peak at 3200 cm^{-1} is a water peak associated with ice formation on the external IR detector. These spectra confirm that decomposition of the 6FDA-DAM:DABA (2:1) free acid polymer does not begin until 470 °C. Since the annealing protocols only go up to 389 °C, carbon formation from polymer decomposition is not responsible for the observed insolubility and plasticization resistance of the rapidly quenched free acid.

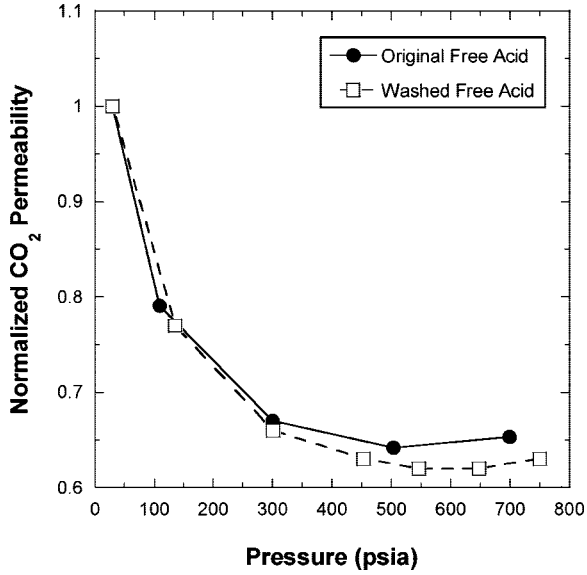

Figure 6. Normalized CO_2 permeability for the washed and original free acid polymer following rapid quenching from above T_G.

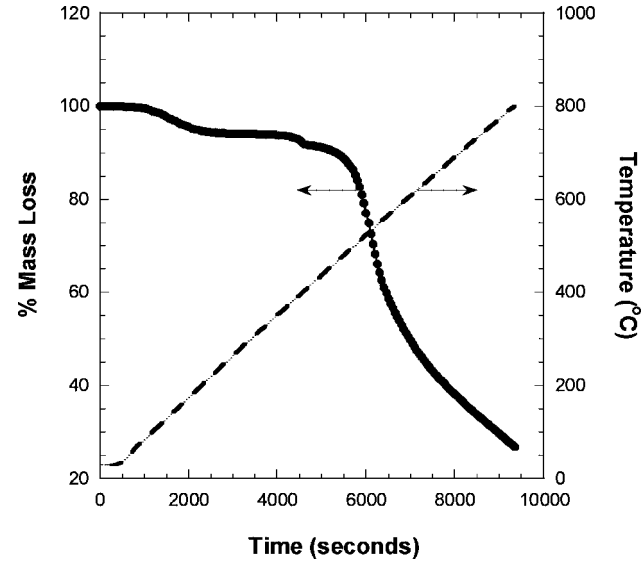

Figure 7. % Mass loss and temperature profile of TGA measurement of the 6FDA-DAM:DABA (2:1) free acid polymer for decomposition characterization.

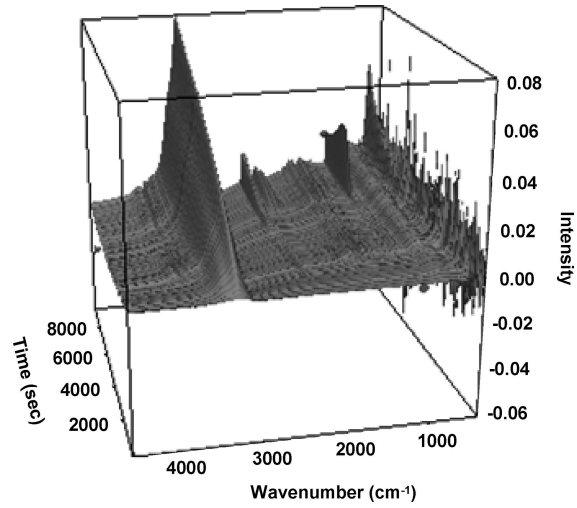

Figure 8. 3-D IR spectrum of evolved gases for the 800 °C TGA of the free acid.

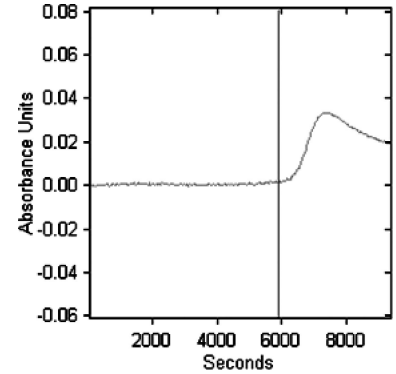

Figure 9. IR trace of 1150 cm^{-1} from the above 3-D IR spectrum. This wavelength is associated with HCF_3 evolution during decomposition.

Investigation of Anhydride Formation. Previous work with polymethacrylates and poly(mono-*n*-akyl itaconates) have discovered the presence of anhydride formation at carboxylic acid sites as one of the first steps of thermal degradation.[22−27] These formations occur as increased chain mobility at higher temp-

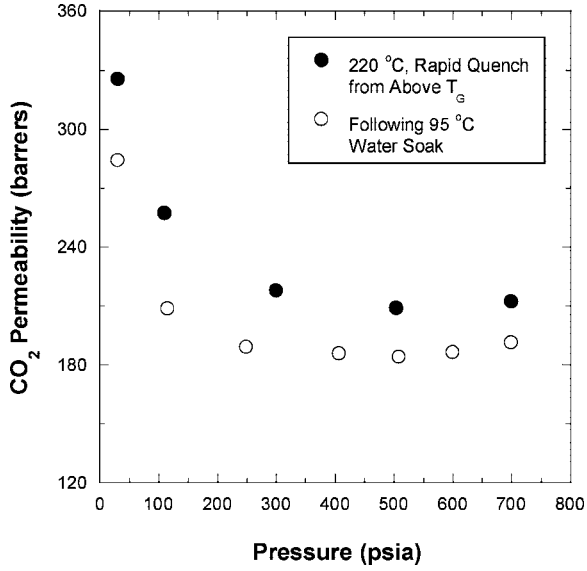

Figure 10. CO_2 permeation isotherm of a free acid film rapidly quenched from above T_G and then conditioned overnight in 95 °C water.

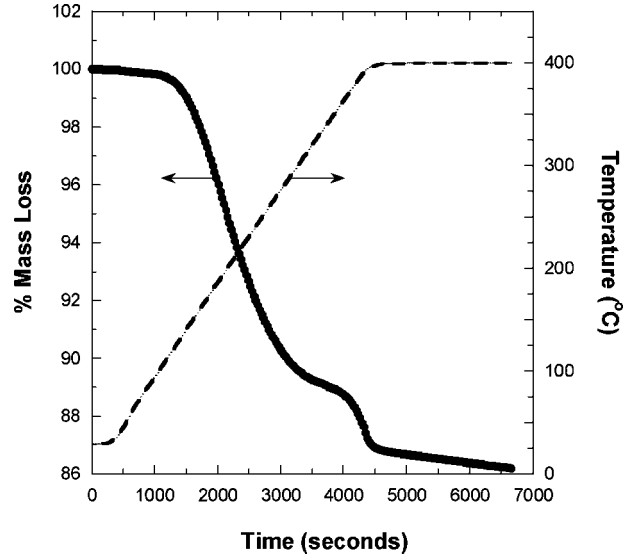

Figure 11. Percent mass loss and temperature profile of a free acid film to mimic the annealing protocol above T_G.

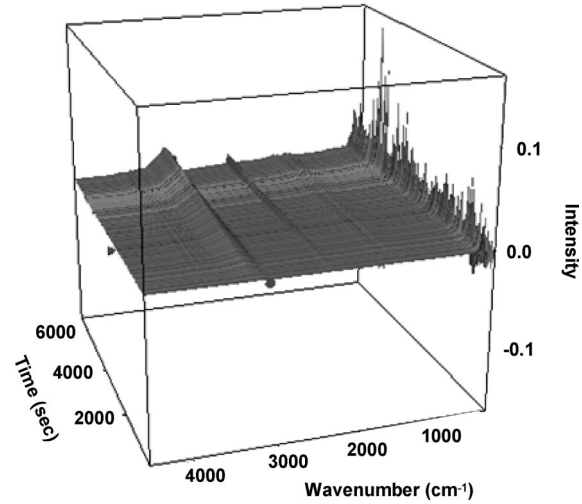

Figure 12. 3-D IR spectra of evolved gases corresponding to the TGA run in Figure 11.

eratures allows alignment of the acid site and subsequent anhydride formation with the loss of water. Velada et al. concluded that linear, intermolecular anhydride formation was responsible for polymer cross-linking and resulting insolubility in typical solvents,[26] and many other studies have shown that intermolecular anhydride formation can occur in these polymers.[22,23,25] Also, upon further heating, these anhydrides have been shown to release CO_2 and form a ketone cross-link.[24,25] The presence of the carboxylic acid site on the DABA moiety lends the possibility of these same anhydride formations to create intramolecular or intermolecular cross-links.

Unfortunately, IR wavelengths typically associated with anhydride formation, 3600−2500, 1795, 1750, and 1022 cm^{-1}, are coupled with other structures in the free acid and are not independently discernible following the rapid quench from above T_G. Therefore, IR cannot be used to detect these formations. However, the doubly conjugated benzophenone, which would result from the decomposition of the anhydride between two DABA groups, has an IR absorbance near 1680−1640 cm^{-1} which is not present in the free acid spectrum.[28] To determine whether anhydride formations are occurring in the free acid, however, an experiment was performed to hydrolyze the possible anhydride and return the polymer to the previous un-cross-linked state. To do this, a previous free acid film that was rapidly quenched from above T_G was placed in 95 °C water for 8 h in an attempt to hydrolyze any cross-links that may have formed. Following the high-temperature water conditioning, a CO_2 permeation isotherm was performed to determine whether the enhanced plasticization resistance deteriorated to the typical un-cross-linked response. Figure 10 presents the CO_2 permeation results of the rapidly quenched film and the same film after the water conditioning.

The decrease in all permeabilities following water conditioning is a result of physical aging of the film. Approximately 2 months elapsed between the rapid quench and water treatment. This rigorous water treatment should be sufficient to hydrolyze any anhydride formation; however, the plasticization resistance following the treatment is nearly identical to that following rapid quench from above T_G. Figure 3 presents the CO_2 permeation isotherm of an un-cross-linked free acid film, and there is a clear upswing in the CO_2 permeability at ∼400 psia which is not apparent in the water-treated permeation isotherm. If anhydride formation does occur without any subsequent reactions when the free acid is annealed above T_G, it is most likely eliminated following the rapid quench and does not play a role in the observed insolubility effects and plasticization resistance.

Decarboxylation of the DABA Moiety. Figure 7 displayed a small mass loss in the free acid that begins at ∼350 °C. To determine whether this loss occurs in a free acid film that is annealed using protocol 1, a free acid film was measured using a TGA program that mimics the annealing protocol, albeit with a slower ramp. The ramp rate was maintained at 5 °C/min, and the film was heated to 390 °C and held at that temperature for 40 min. The TGA mass loss for this run is presented in Figure 11.

This TGA profile clearly shows a mass loss at 350 °C that continues until the 390 °C isothermal stage is reached. This temperature falls in the range attributed to decarboxylation as observed in acid-containing polymers such as acrylic acid and poly(*p*-methylacryloyloxybenzoic acid).[27,29] In the decarboxylation process, CO_2 and/or CO are evolved in gas form. Figures 12 and 13 display the 3-D IR spectra of gas evolution and IR trace at 2354 cm^{-1} which is associated with CO_2 evolution. No CO evolution was detected by IR as an evolved gas. Again, the large peak at 3200 cm^{-1} is a water peak associated with ice formation on the external IR detector; however, it is still possible

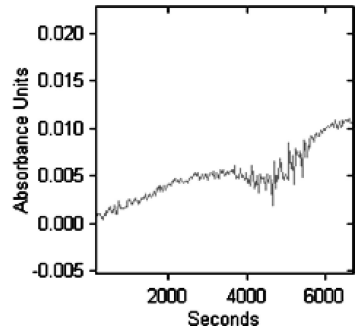

Figure 13. IR trace of 2354 cm^{-1} from the above 3-D IR spectrum.

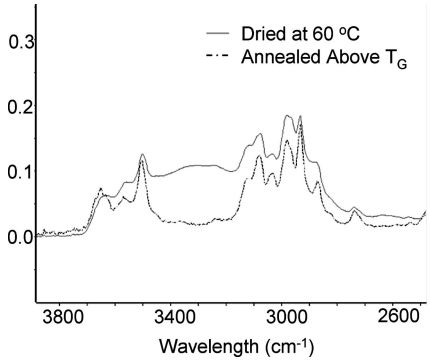

Figure 14. High-frequency IR spectra of a dried free acid film and a free acid film annealed above T_G.

that water is evolved during this process, and the signal is hidden within this large peak. The increase in absorbance during the first 2500 s in Figure 13 is not fully understood at this time; however, it could be sorbed CO_2 within the polymer that is evolved as temperature increases. However, there is a distinct increase in the absorbance beginning at ~4500 s, which corresponds to the significant mass loss that occurs between 4000 and 4500 s in Figure 11. Therefore, CO_2 is most likely being evolved from the polymer during this portion of the thermal treatment. As a means of confirming that the carboxylic acid group is responsible for this mass loss, a TGA profile of the 6FDA-DAM polymer was conducted, and there is no mass loss prior to the major decomposition of the polymer.

Cervantes et al. concluded that benzoic anhydride is first formed at lower temperatures and the CO_2 evolution that occurs at 353 °C is the result of decarboxylation of the anhydride structures.[27] If the free acid polymer followed a similar process, the mass loss associated with removal of the complete anhydride structure from the polymer is 2.16% per 2 repeat units of the free acid (6 6FDA, 4 DAM, 2 DABA). This value takes into account water removal at lower temperatures to form the anhydride. A first-derivative analysis of the TGA data in Figure 11 confirms a mass loss of 2.0% at this step. This result substantiates the possibility that the observed mass loss at temperatures just below T_G for the free acid polymer is associated with the decarboxylation of the free acid in the DABA species.

IR spectra of a dried free acid film and a film quenched from above T_G also indicate the significant loss of these acid sites. Figure 14 displays the high-frequency range for these films, and the broad peaks in the range of 3700−3100 cm^{-1} typically associated with OH stretching vibrations have been greatly diminished in the film annealed above T_G. This broad peak range is not just a result of sorbed water in the polymer since the film annealed above T_G was rapidly quenched to room conditions and was not measured with IR for a number of days. Therefore, it would have reached equilibrium with the environment just as the dried free acid film.

Table 2. Ratio of Peak Areas with Respect to the Aromatic/CF_3 Peak Areas

C NMR peak	220 °C	220 °C (quench from above T_G)	% change
carbonyl carbon (173−160 ppm)	0.192	0.161	16.1
quaternary carbon (69−53 ppm)	0.084	0.083	1.2
methyl carbon (22−2 ppm)	0.300	0.305	−1.6

C NMR was conducted on the free acid polymer to confirm the loss of the carboxylic acid carbon during the heat treatment above T_G. A free acid sample dried at 220 °C was compared to a sample thermally treated using protocol 2. All chemical shift assignments were determined using ChemDraw software. Because the absolute intensities of the spectra are not equivalent, all data analysis is conducted with respect to the aromatic/CF_3 peaks of the polymer in the range of 150−105 ppm. The peak of interest is the carbonyl carbon band in the range of 170−160 ppm, which comprises the carboxylic acid carbons as well as the imide carbonyl carbons. An integral analysis of the peaks confirms a reduction in the carbonyl carbon peak following annealing above T_G. To ensure this technique is accurate, peak integral analyses for the quaternary carbon attached to the CF_3 groups and the methyl carbons from the DAM diamine with respect to the aromatic/CF_3 peak were also measured. These results are displayed in Table 2. Since there is one carboxylic acid carbon and eight imide carbonyl carbons in a repeat unit, the theoretical loss for complete decarboxylation is only 11.1%. While it is not possible to definitively determine the uncertainty associated with this measurement technique, the percent change of the quaternary carbon and methyl carbon peaks sheds some light on the uncertainty of these measurements. At the very least, this technique establishes the fact that a C═O carbon is being removed from the polymer structure when the free acid polymer is annealed above T_G.

Possible Mechanism of Covalent Cross-Linking of the Free Acid. Decarboxylation studies of aromatic carboxylic acids have been performed in the past to gain an understanding of how the process occurs and if it can lead to cross-linking during the thermal processing of low rank coals.[30−32] In one study using a neutral environment, Eskay et al. conclude that the cross-linking of a model acid occurs through anhydride formation and subsequent decomposition to form aryl radicals which cross-link with the naphthalene solvent. In fact, thermolysis of the model anhydride in naphthalene yielded 57% cross-linked products with a decomposition rate of 88% h^{-1} at 400 °C.[32] Interestingly, there was no cross-linked product created from two model acids forming a bond at the open radical sites. On the basis of the reaction products and gas byproducts, Eskay et al. concluded that the decomposition of the anhydride was most likely induced by a radical and not a result of homolysis of the C(═O)−O bond.

As shown earlier, the amount of mass loss in the 6FDA-DAM:DABA (2:1) free acid polymer at 350 °C is slightly below the theoretical amount of complete removal of the anhydride formation across two DABA species. With the known pathway to cross-linking shown to occur in the model acid described above, it is reasonable to conclude that the high-temperature treatment of the 6FDA-DAM:DABA (2:1) free acid polymer produces a cross-linked polymer in which the acid site of the DABA group is arylated to another portion of the polymer backbone. This cross-linking most likely occurs in a few different places along the backbone. If the proposed induced decomposition pathway of the anhydride holds true, then a hydrogen must be abstracted from the backbone. The hydrogens in the DAM methyl groups have the lowest bond dissociation

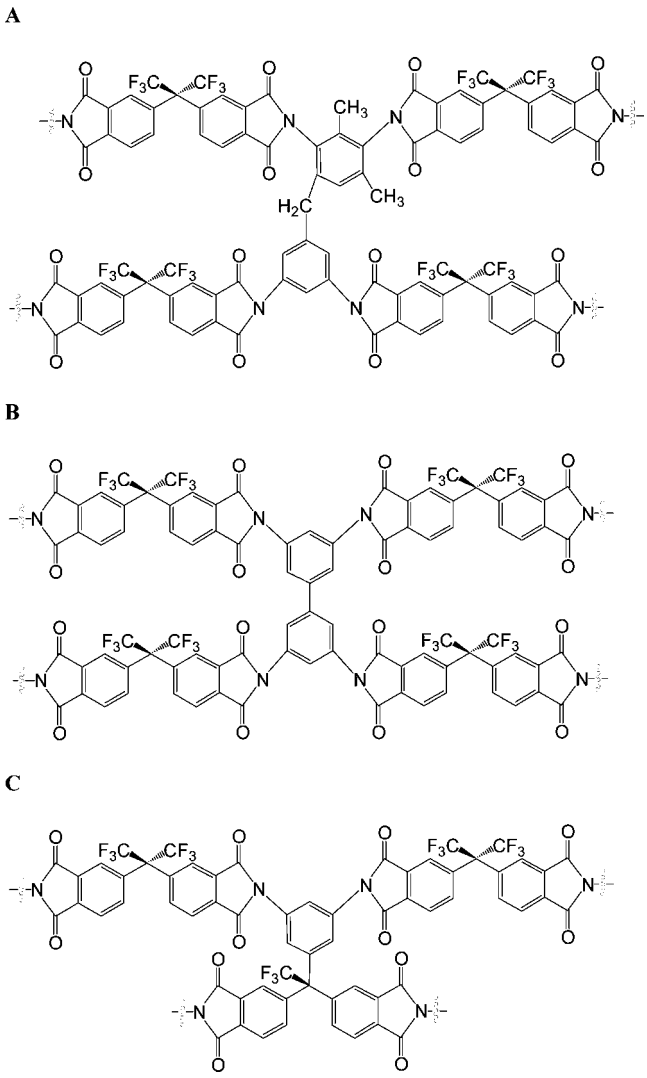

Figure 15. Possible cross-linking sites through the diamines in the free acid polymer: (A) through the DAM methyl, (B) biphenyl cross-link, and (C) at the cleaved CF_3 site.

energy and are therefore most likely to be abstracted, which then creates a methyl radical and possible cross-linking site.[33] Conversely, even though Eskay et al. did not observe any cross-linked model acids, it may be possible for two radical DABA groups to form linkage and corresponding biphenyl. One other possibility exists as a potential cross-linking point. The gradual mass loss at 389 °C from 4500 to 6500 s in Figure 5.9 may be the onset of decomposition caused by HCF_3 loss. A similar TGA experiment was conducted with a maximum temperature of 450 °C. In this run, the gradual mass loss at the isothermal step was slightly enhanced, and the IR spectrum of evolved gases exhibited a small peak at 1149 cm^{-1} which is indicative of HCF_3 evolution. Therefore, it is possible that a small number of the CF_3 groups are being cleaved at 389 °C. The leaving CF_3 group would then provide an available radical site for cross-linking. While this structure appears to be too sterically hindered to form, there have been studies conducted with a structurally similar polymer.[34,35] The structures of these proposed cross-linking sites are shown in Figure 15.

These proposed points of cross-linking would not significantly alter the IR signature of the polymer, which is consistent with what is observed as shown in Figure 16. The only substantial difference between these spectra is the diminished peak at 1400 cm^{-1} in the film annealed above T_G. While this peak is not

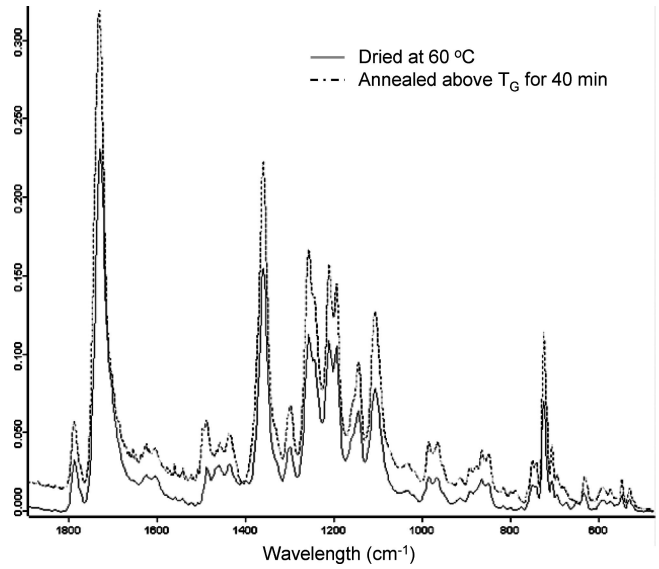

Figure 16. IR spectra comparing the free acid before and after annealing above T_G.

definitively known, it may be the OH in-plane deformation of carboxyl dimers which ranges from 1440 to 1395 cm^{-1}.[28]

Conclusions

Upon rapid quenching from above T_G, the 6FDA-DAM:DABA (2:1) free acid polymer exhibits unusual responses for a polymer simply annealed above T_G. The polymer becomes insoluble in strong solvents and exhibits excellent plasticization resistance in CO_2, indicating some form of cross-linking has occurred. Charge transfer complexes, oligomer cross-linking, anhydride cross-linking, and bulk decomposition are all dismissed as possible causes for these observed responses. TGA-IR and C NMR measurements confirm the free acid in the polymer undergoes decarboxylation just prior to reaching the T_G. The subsequent aryl radicals then cross-link with a few proposed sites along the polymer backbone. The resulting aliphatic and aryl cross-links provide a much more robust polymer material for membrane separations.

Acknowledgment. The authors of this paper thank Dr. Carsten Sievers for assistance with C NMR measurements. This research has been supported by the United States Department of Energy Grant DE-FG03-95ER14538.

References and Notes

(1) Ohya, H.; Kudryavtsev, V. V.; Semenova, S. I. *Polyimide Membranes: Applications, Fabrications, and Properties*; Kodansha Ltd.: Tokyo, 1996.
(2) Wind, J. D.; Staudt-Bickel, C.; Paul, D. R.; Koros, W. J. *Macromolecules* **2003**, *36*, 1882–1888.
(3) Wind, J. D.; Staudt-Bickel, C.; Paul, D. R.; Koros, W. J. *Ind. Eng. Chem. Res.* **2002**, *41*, 6139–6148.
(4) Wind, J. D.; Paul, D. R.; Koros, W. J. *J. Membr. Sci.* **2004**, *228*, 227–236.
(5) Hillock, A. M. W.; Koros, W. J. *Macromolecules* **2007**, *40*, 583–587.
(6) Wallace, D. W.; Williams, J.; Staudt-Bickel, C.; Koros, W. J. *Polymer* **2006**, *47*, 1207–1216.
(7) Thundyil, M. J.; Jois, Y. H.; Koros, W. K. *J. Membr. Sci.* **1999**, *152*, 29–40.
(8) Wind, J. D. *Improving Polyimide Membrane Resistance to Carbon Dioxide Plasticization in Natural Gas Separations*; University of Texas-Austin: Austin, TX, 2002.
(9) Kim, J. H.; Koros, W. J.; Paul, D. R. *Polymer* **2006**, *47*, 3094–3103.
(10) Bos, A.; Punt, I. G. M.; Wessling, M.; Strathmann, H. *Sep. Purif. Technol.* **1998**, *14*, 27–39.
(11) Barsema, J. N.; Klijnstra, S. D.; Balster, J. H.; van der Vegt, N. F. A.; Koops, G. H.; Wessling, M. *J. Membr. Sci.* **2004**, *238*, 93–102.

(12) Zhou, F. B.; Koros, W. J. *Polymer* **2006**, *47*, 280–288.
(13) Steel, K. M.; Koros, W. J. *Carbon* **2003**, *41*, 253–266.
(14) Steel, K. M.; Koros, W. J. *Carbon* **2005**, *43*, 1843–1856.
(15) Vu, D. Q.; Miller, S. J.; Koros, W. J. *Ind. Eng. Chem. Res.* **2002**, *41*, 367–380.
(16) Huang, Y.; Paul, D. R. *Macromolecules* **2005**, *38*, 10148–10154.
(17) Liu, Y.; Chng, M. L.; Chung, T. S.; Wang, R. *J. Membr. Sci.* **2003**, *214*, 83–92.
(18) Cao, C.; Chung, T. S.; Liu, Y.; Wang, R.; Pramoda, K. P. *J. Membr. Sci.* **2003**, *216*, 257–268.
(19) Shao, L.; Chung, T. S.; Goh, S. H.; Pramoda, K. P. *J. Membr. Sci.* **2004**, *238*, 153–163.
(20) Shao, L.; Chung, T. S.; Goh, S. H.; Pramoda, K. P. *J. Membr. Sci.* **2005**, *256*, 46–56.
(21) Williams, P. J. *Analysis of Factors Influencing the Performance of CMS Membranes for Gas Separation*, Georgia Institute of Technology, **2007**.
(22) Grant, D. G.; Grassie, N. *Polymer* **1960**, *1*, 125–134.
(23) McGaugh, M. C.; Kottle, S. *Polym. Lett.* **1967**, *5*, 817–820.
(24) Maurer, J. J.; Eustace, D. J.; Ratcliffe, C. T. *Macromolecules* **1987**, *20*, 196–202.
(25) Ho, B. C.; Lee, Y. D.; Chin, W. K. *J. Polym. Sci., Part A: Polym. Chem.* **1992**, *30*, 2389–2397.
(26) Velada, J. L.; Carlos, C.; Madoz, A.; Katime, I. *Macromol. Chem. Phys.* **1995**, *196*, 3171–3185.
(27) Cervantes-Uc, J. M.; Cauich-Rodriguez, J. V.; Vazquez-Torres, H.; Licea-Claverie, A. *Polym. Degrad. Stab.* **2006**, *91*, 3312–3321.
(28) Colthup, N. B.; Daly, L. H.; Wiberley, S. E. *Introduction to Infrared and Raman Spectroscopy*; Academic Press: San Diego, 1990.
(29) Giroux, L.; Charland, J. P.; MacPhee, J. A. *Energy Fuels* **2006**, *20*, 1988–1996.
(30) Eskay, T. P.; Britt, P. F.; Buchanan, A. C. *Energy Fuels* **1996**, *10*, 1257–1261.
(31) Manion, J. A.; McMillen, D. F.; Malhotra, R. *Energy Fuels* **1996**, *10*, 776–788.
(32) Eskay, T. P.; Britt, P. F.; Buchanan, A. C. *Energy Fuels* **1997**, *11*, 1278–1287.
(33) McMillen, D. F.; Golden, D. M. *Annu. Rev. Phys. Chem.* **1982**, *33*, 493–532.
(34) Plummer, C. J. G.; Hedrick, J. L.; Kausch, H. H.; Hilborn, J. G. *J. Polym. Sci., Part B: Polym. Phys.* **1995**, *33*, 1813–1820.
(35) Hsiao, S. H.; Chen, W. T. *J. Polym. Sci., Part A: Polym. Chem.* **2003**, *41*, 914–921.

MA801586F